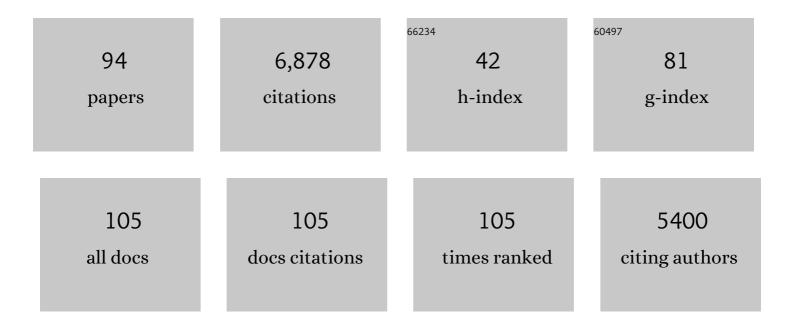
List of Publications by Year in descending order

Source: https://exaly.com/author-pdf/1574486/publications.pdf Version: 2024-02-01



#	Article	IF	CITATIONS
1	Global and time-resolved monitoring of crop photosynthesis with chlorophyll fluorescence. Proceedings of the National Academy of Sciences of the United States of America, 2014, 111, E1327-33.	3.3	741
2	Ecosystem resilience despite large-scale altered hydroclimatic conditions. Nature, 2013, 494, 349-352.	13.7	450
3	Integrating satellite and climate data to predict wheat yield in Australia using machine learning approaches. Agricultural and Forest Meteorology, 2019, 274, 144-159.	1.9	319
4	Recent global decline of CO ₂ fertilization effects on vegetation photosynthesis. Science, 2020, 370, 1295-1300.	6.0	317
5	The seasonal cycle of satellite chlorophyll fluorescence observations and its relationship to vegetation phenology and ecosystem atmosphere carbon exchange. Remote Sensing of Environment, 2014, 152, 375-391.	4.6	287
6	Estimation of vegetation photosynthetic capacity from spaceâ€based measurements of chlorophyll fluorescence for terrestrial biosphere models. Global Change Biology, 2014, 20, 3727-3742.	4.2	260
7	Improving the monitoring of crop productivity using spaceborne solarâ€induced fluorescence. Global Change Biology, 2016, 22, 716-726.	4.2	240
8	Satellite chlorophyll fluorescence measurements reveal largeâ€scale decoupling of photosynthesis and greenness dynamics in boreal evergreen forests. Global Change Biology, 2016, 22, 2979-2996.	4.2	225
9	Model-based analysis of the relationship between sun-induced chlorophyll fluorescence and gross primary production for remote sensing applications. Remote Sensing of Environment, 2016, 187, 145-155.	4.6	185
10	Canopy structure explains the relationship between photosynthesis and sun-induced chlorophyll fluorescence in crops. Remote Sensing of Environment, 2020, 241, 111733.	4.6	183
11	Consistency between sun-induced chlorophyll fluorescence and gross primary production of vegetation in North America. Remote Sensing of Environment, 2016, 183, 154-169.	4.6	180
12	Characteristics and factors controlling the development of ephemeral gullies in cultivated catchments of black soil region, Northeast China. Soil and Tillage Research, 2007, 96, 28-41.	2.6	163
13	Satellite sunâ€induced chlorophyll fluorescence detects early response of winter wheat to heat stress in the Indian Indoâ€Gangetic Plains. Global Change Biology, 2018, 24, 4023-4037.	4.2	152
14	Chlorophyll fluorescence tracks seasonal variations of photosynthesis from leaf to canopy in a temperate forest. Global Change Biology, 2017, 23, 2874-2886.	4.2	135
15	Tracking the seasonal and inter-annual variations of global gross primary production during last four decades using satellite near-infrared reflectance data. Science of the Total Environment, 2021, 755, 142569.	3.9	125
16	Estimating crop primary productivity with Sentinel-2 and Landsat 8 using machine learning methods trained with radiative transfer simulations. Remote Sensing of Environment, 2019, 225, 441-457.	4.6	112
17	Development of gullies and sediment production in the black soil region of northeastern China. Geomorphology, 2008, 101, 683-691.	1.1	103
18	Projected rainfall erosivity changes under climate change from multimodel and multiscenario projections in Northeast China. Journal of Hydrology, 2010, 384, 97-106.	2.3	98

#	Article	IF	CITATIONS
19	Urbanâ°'rural gradients reveal joint control of elevated CO2 and temperature on extended photosynthetic seasons. Nature Ecology and Evolution, 2019, 3, 1076-1085.	3.4	98
20	On the relationship between sub-daily instantaneous and daily total gross primary production: Implications for interpreting satellite-based SIF retrievals. Remote Sensing of Environment, 2018, 205, 276-289.	4.6	91
21	Chlorophyll a fluorescence illuminates a path connecting plant molecular biology to Earth-system science. Nature Plants, 2021, 7, 998-1009.	4.7	88
22	Drought rapidly diminishes the large net CO2 uptake in 2011 over semi-arid Australia. Scientific Reports, 2016, 6, 37747.	1.6	83
23	Reduction of structural impacts and distinction of photosynthetic pathways in a global estimation of GPP from space-borne solar-induced chlorophyll fluorescence. Remote Sensing of Environment, 2020, 240, 111722.	4.6	83
24	Comparison of solarâ€induced chlorophyll fluorescence, lightâ€use efficiency, and processâ€based <scp>GPP</scp> models in maize. Ecological Applications, 2016, 26, 1211-1222.	1.8	82
25	Solar-induced chlorophyll fluorescence and its link to canopy photosynthesis in maize from continuous ground measurements. Remote Sensing of Environment, 2020, 236, 111420.	4.6	81
26	NIRVP: A robust structural proxy for sun-induced chlorophyll fluorescence and photosynthesis across scales. Remote Sensing of Environment, 2022, 268, 112763.	4.6	77
27	Functional response of U.S. grasslands to the early 21stâ€century drought. Ecology, 2014, 95, 2121-2133.	1.5	75
28	Extreme precipitation patterns and reductions of terrestrial ecosystem production across biomes. Journal of Geophysical Research G: Biogeosciences, 2013, 118, 148-157.	1.3	74
29	Short-term gully retreat rates over rolling hill areas in black soil of Northeast China. Catena, 2007, 71, 321-329.	2.2	71
30	Progress and Trends in the Application of Google Earth and Google Earth Engine. Remote Sensing, 2021, 13, 3778.	1.8	71
31	Spatially-explicit monitoring of crop photosynthetic capacity through the use of space-based chlorophyll fluorescence data. Remote Sensing of Environment, 2018, 210, 362-374.	4.6	69
32	FluoSpec 2—An Automated Field Spectroscopy System to Monitor Canopy Solar-Induced Fluorescence. Sensors, 2018, 18, 2063.	2.1	67
33	Satellite-based survey of extreme methane emissions in the Permian basin. Science Advances, 2021, 7, .	4.7	66
34	Angle matters: Bidirectional effects impact the slope of relationship between gross primary productivity and sunâ€induced chlorophyll fluorescence from Orbiting Carbon Observatoryâ€2 across biomes. Global Change Biology, 2018, 24, 5017-5020.	4.2	62
35	An Overview of the Applications of Earth Observation Satellite Data: Impacts and Future Trends. Remote Sensing, 2022, 14, 1863.	1.8	61
36	Modeling canopy conductance and transpiration from solar-induced chlorophyll fluorescence. Agricultural and Forest Meteorology, 2019, 268, 189-201.	1.9	60

#	Article	IF	CITATIONS
37	From Canopyâ€Leaving to Total Canopy Farâ€Red Fluorescence Emission for Remote Sensing of Photosynthesis: First Results From TROPOMI. Geophysical Research Letters, 2019, 46, 12030-12040.	1.5	59
38	The TROPOSIF global sun-induced fluorescence dataset from the Sentinel-5P TROPOMI mission. Earth System Science Data, 2021, 13, 5423-5440.	3.7	54
39	Spatioâ€Temporal Convergence of Maximum Daily Lightâ€Use Efficiency Based on Radiation Absorption by Canopy Chlorophyll. Geophysical Research Letters, 2018, 45, 3508-3519.	1.5	48
40	Warmer spring alleviated the impacts of 2018 European summer heatwave and drought on vegetation photosynthesis. Agricultural and Forest Meteorology, 2020, 295, 108195.	1.9	48
41	Photoperiod decelerates the advance of spring phenology of six deciduous tree species under climate warming. Global Change Biology, 2021, 27, 2914-2927.	4.2	48
42	SIFSpec: Measuring Solar-Induced Chlorophyll Fluorescence Observations for Remote Sensing of Photosynthesis. Sensors, 2019, 19, 3009.	2.1	44
43	Advances in hyperspectral remote sensing of vegetation traits and functions. Remote Sensing of Environment, 2021, 252, 112121.	4.6	44
44	Satellite evidence for China's leading role in restoring vegetation productivity over global karst ecosystems. Forest Ecology and Management, 2022, 507, 120000.	1.4	44
45	Separating the effects of climate change and human activity on water use efficiency over the Beijing-Tianjin Sand Source Region of China. Science of the Total Environment, 2019, 690, 584-595.	3.9	43
46	Assessing bi-directional effects on the diurnal cycle of measured solar-induced chlorophyll fluorescence in crop canopies. Agricultural and Forest Meteorology, 2020, 295, 108147.	1.9	43
47	Satellite Chlorophyll Fluorescence and Soil Moisture Observations Lead to Advances in the Predictive Understanding of Global Terrestrial Coupled Carbonâ€Water Cycles. Global Biogeochemical Cycles, 2018, 32, 360-375.	1.9	42
48	Response of Ecosystem Water Use Efficiency to Drought over China during 1982–2015: Spatiotemporal Variability and Resilience. Forests, 2019, 10, 598.	0.9	42
49	The potential of satellite FPAR product for GPP estimation: An indirect evaluation using solar-induced chlorophyll fluorescence. Remote Sensing of Environment, 2020, 240, 111686.	4.6	42
50	A model for estimating transpiration from remotely sensed solar-induced chlorophyll fluorescence. Remote Sensing of Environment, 2021, 252, 112134.	4.6	39
51	Distinguishing Anthropogenic CO ₂ Emissions From Different Energy Intensive Industrial Sources Using OCOâ€2 Observations: A Case Study in Northern China. Journal of Geophysical Research D: Atmospheres, 2018, 123, 9462-9473.	1.2	36
52	Simulating emission and scattering of solar-induced chlorophyll fluorescence at far-red band in global vegetation with different canopy structures. Remote Sensing of Environment, 2019, 233, 111373.	4.6	36
53	The characteristics of gully erosion over rolling hilly black soil areas of Northeast China. Journal of Chinese Geography, 2009, 19, 309-320.	1.5	29
54	Variations and drivers of methane fluxes from a rice-wheat rotation agroecosystem in eastern China at seasonal and diurnal scales. Science of the Total Environment, 2019, 690, 973-990.	3.9	29

#	Article	IF	CITATIONS
55	Satellite-observed solar-induced chlorophyll fluorescence reveals higher sensitivity of alpine ecosystems to snow cover on the Tibetan Plateau. Agricultural and Forest Meteorology, 2019, 271, 126-134.	1.9	29
56	Satellite-Observed Variations and Trends in Carbon Monoxide over Asia and Their Sensitivities to Biomass Burning. Remote Sensing, 2020, 12, 830.	1.8	26
57	Wide discrepancies in the magnitude and direction of modeled solar-induced chlorophyll fluorescence in response to light conditions. Biogeosciences, 2020, 17, 3733-3755.	1.3	24
58	Widespread Decline in Vegetation Photosynthesis in Southeast Asia Due to the Prolonged Drought During the 2015/2016 El Niño. Remote Sensing, 2019, 11, 910.	1.8	23
59	ChinaSpec: A Network for Longâ€Term Groundâ€Based Measurements of Solarâ€Induced Fluorescence in China. Journal of Geophysical Research G: Biogeosciences, 2021, 126, e2020JG006042.	1.3	22
60	Comparative rates of wind versus water erosion from a small semiarid watershed in southern Arizona, USA. Aeolian Research, 2011, 3, 197-204.	1.1	20
61	Sensitivity of Estimated Total Canopy SIF Emission to Remotely Sensed LAI and BRDF Products. Journal of Remote Sensing, 2021, 2021, .	3.2	20
62	Intermediate Aerosol Loading Enhances Photosynthetic Activity of Croplands. Geophysical Research Letters, 2021, 48, e2020GL091893.	1.5	19
63	Seasonal variations in the relationship between sun-induced chlorophyll fluorescence and photosynthetic capacity from the leaf to canopy level in a rice crop. Journal of Experimental Botany, 2020, 71, 7179-7197.	2.4	18
64	Performance of a two-leaf light use efficiency model for mapping gross primary productivity against remotely sensed sun-induced chlorophyll fluorescence data. Science of the Total Environment, 2018, 613-614, 977-989.	3.9	17
65	Tracking Seasonal and Interannual Variability in Photosynthetic Downregulation in Response to Water Stress at a Temperate Deciduous Forest. Journal of Geophysical Research G: Biogeosciences, 2020, 125, e2018JG005002.	1.3	17
66	The Ability of Sun-Induced Chlorophyll Fluorescence From OCO-2 and MODIS-EVI to Monitor Spatial Variations of Soybean and Maize Yields in the Midwestern USA. Remote Sensing, 2020, 12, 1111.	1.8	17
67	Assessing phenological change in China from 1982 to 2006 using AVHRR imagery. Frontiers of Earth Science, 2012, 6, 227-236.	0.9	16
68	Comparison of Bi-Hemispherical and Hemispherical-Conical Configurations for In Situ Measurements of Solar-Induced Chlorophyll Fluorescence. Remote Sensing, 2019, 11, 2642.	1.8	16
69	Correcting Clearâ€Sky Bias in Gross Primary Production Modeling From Satellite Solarâ€Induced Chlorophyll Fluorescence Data. Journal of Geophysical Research G: Biogeosciences, 2020, 125, e2020JG005822.	1.3	15
70	Response to Comments on "Recent global decline of CO ₂ fertilization effects on vegetation photosynthesis― Science, 2021, 373, eabg7484.	6.0	15
71	Resistance and resilience of grasslands to drought detected by SIF in inner Mongolia, China. Agricultural and Forest Meteorology, 2021, 308-309, 108567.	1.9	15
72	Adjusting solar-induced fluorescence to nadir-viewing provides a better proxy for GPP. ISPRS Journal of Photogrammetry and Remote Sensing, 2022, 186, 157-169.	4.9	14

#	Article	IF	CITATIONS
73	Potential of Sunâ€Induced Chlorophyll Fluorescence for Indicating Mangrove Canopy Photosynthesis. Journal of Geophysical Research G: Biogeosciences, 2021, 126, e2020JG006159.	1.3	13
74	Global assessment of partitioning transpiration from evapotranspiration based on satellite solar-induced chlorophyll fluorescence data. Journal of Hydrology, 2022, 612, 128044.	2.3	13
75	Reply to Magnani et al.: Linking large-scale chlorophyll fluorescence observations with cropland gross primary production. Proceedings of the National Academy of Sciences of the United States of America, 2014, 111, E2511.	3.3	11
76	Constraining global terrestrial gross primary productivity in a global carbon assimilation system with OCO-2 chlorophyll fluorescence data. Agricultural and Forest Meteorology, 2021, 304-305, 108424.	1.9	10
77	Exploring Seasonal and Circadian Rhythms in Structural Traits of Field Maize from LiDAR Time Series. Plant Phenomics, 2021, 2021, 9895241.	2.5	10
78	Physiological dynamics dominate the response of canopy far-red solar-induced fluorescence to herbicide treatment. Agricultural and Forest Meteorology, 2022, 323, 109063.	1.9	10
79	Simulation of solar-induced chlorophyll fluorescence in a heterogeneous forest using 3-D radiative transfer modelling and airborne LiDAR. ISPRS Journal of Photogrammetry and Remote Sensing, 2022, 191, 1-17.	4.9	7
80	Evaluating Multi-Angle Photochemical Reflectance Index and Solar-Induced Fluorescence for the Estimation of Gross Primary Production in Maize. Remote Sensing, 2020, 12, 2812.	1.8	6
81	Resolving temperature limitation on spring productivity in an evergreen conifer forest using a model–data fusion framework. Biogeosciences, 2022, 19, 541-558.	1.3	6
82	Recent advances in global monitoring of terrestrial sun-induced chlorophyll fluorescence. , 2016, , .		5
83	Evaluation of GOFP over four forest plots using RAMI and UAV measurements. International Journal of Digital Earth, 2021, 14, 1433-1451.	1.6	5
84	Temporal resolution of vegetation indices and solar-induced chlorophyll fluorescence data affects the accuracy of vegetation phenology estimation: A study using in-situ measurements. Ecological Indicators, 2022, 136, 108673.	2.6	5
85	The Effects of Sun-Viewer Geometry on Sun-Induced Fluorescence and Its Relationship with Gross Primary Production. , 2019, , .		4
86	Groundâ€Based Multiangle Solarâ€Induced Chlorophyll Fluorescence Observation and Angular Normalization for Assessing Crop Productivity. Journal of Geophysical Research G: Biogeosciences, 2021, 126, e2020JG006082.	1.3	4
87	Seasonal Variations in Leaf Maximum Photosynthetic Capacity and Its Dependence on Climate Factors Across Global FLUXNET Sites. Journal of Geophysical Research G: Biogeosciences, 2022, 127, .	1.3	4
88	Sun-induced chlorophyll fluorescence is more strongly related to photosynthesis with hemispherical than nadir measurements: Evidence from field observations and model simulations. Remote Sensing of Environment, 2022, 279, 113118.	4.6	4
89	Can we retrieve vegetation photosynthetic capacity paramter from solar-induced fluorescence?. , 2016, , .		3
90	LINKING PHOTOSYNTHETIC LIGHT USE EFFICIENCY AND OPTICAL VEGETATION ACTIVE INDICATORS: IMPLICATIONS FOR GROSS PRIMARY PRODUCTION ESTIMATION BY REMOTE SENSING. ISPRS Annals of the Photogrammetry, Remote Sensing and Spatial Information Sciences, 0, V-3-2020, 571-578.	0.0	2

#	Article	IF	CITATIONS
91	Modeling solar-induced fluorescence of forest with heterogeneous distribution of damaged foliage by extending the stochastic radiative transfer theory. Remote Sensing of Environment, 2022, 271, 112892.	4.6	2
92	Influences of fractional vegetation cover on the spatial variability of canopy SIF from unmanned aerial vehicle observations. International Journal of Applied Earth Observation and Geoinformation, 2022, 107, 102712.	1.4	2
93	Fusion of SCIAMACHY and GOME-2 satellite sun-induced fluorescence data. , 2016, , .		1
94	Beyond APAR and NPQ: Factors Coupling and Decoupling SIF and GPP Across Scales. , 2021, , .		0